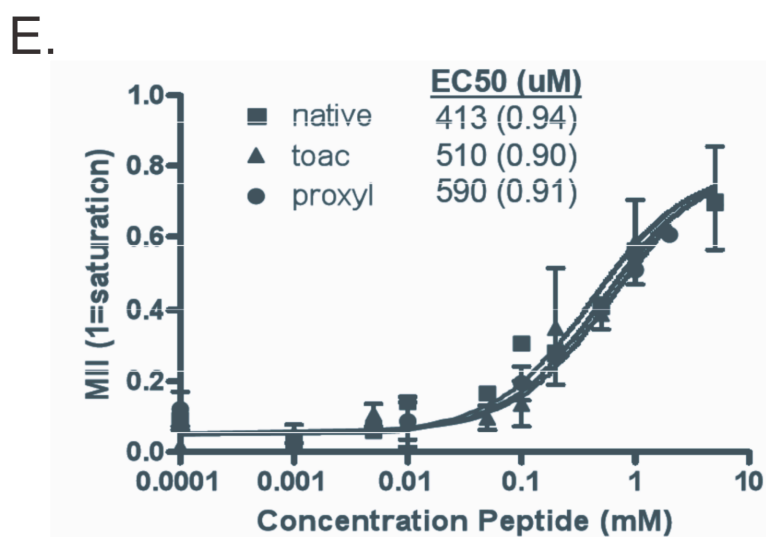
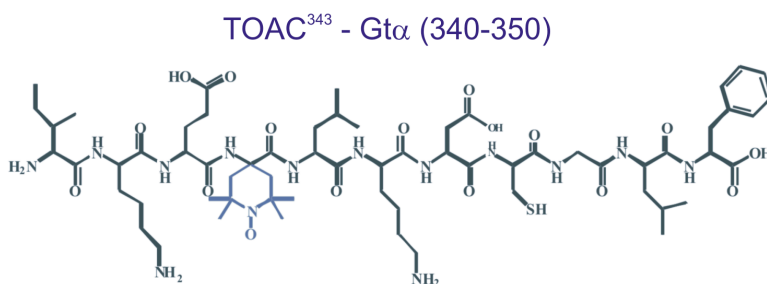
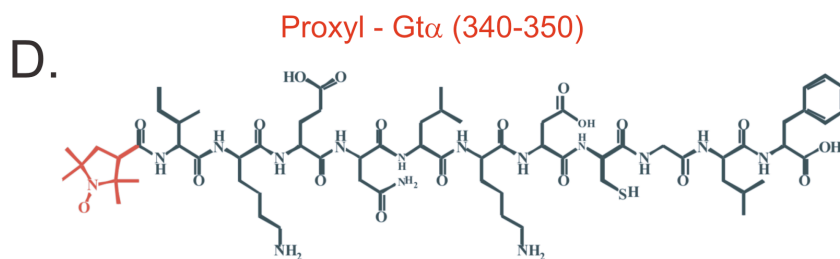
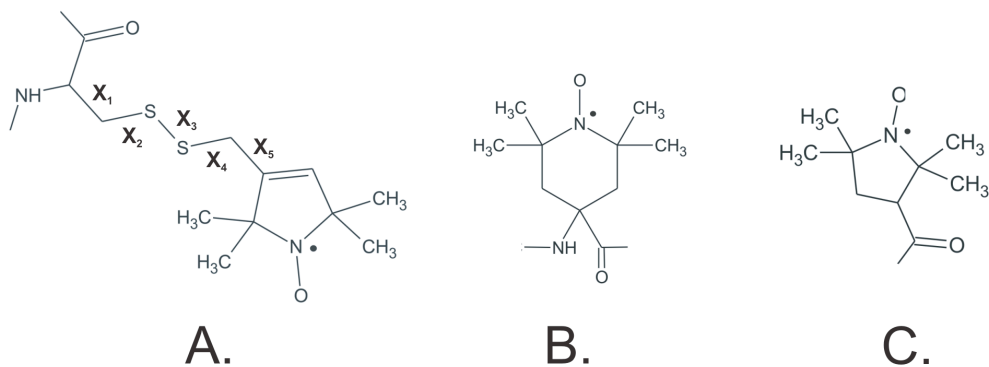
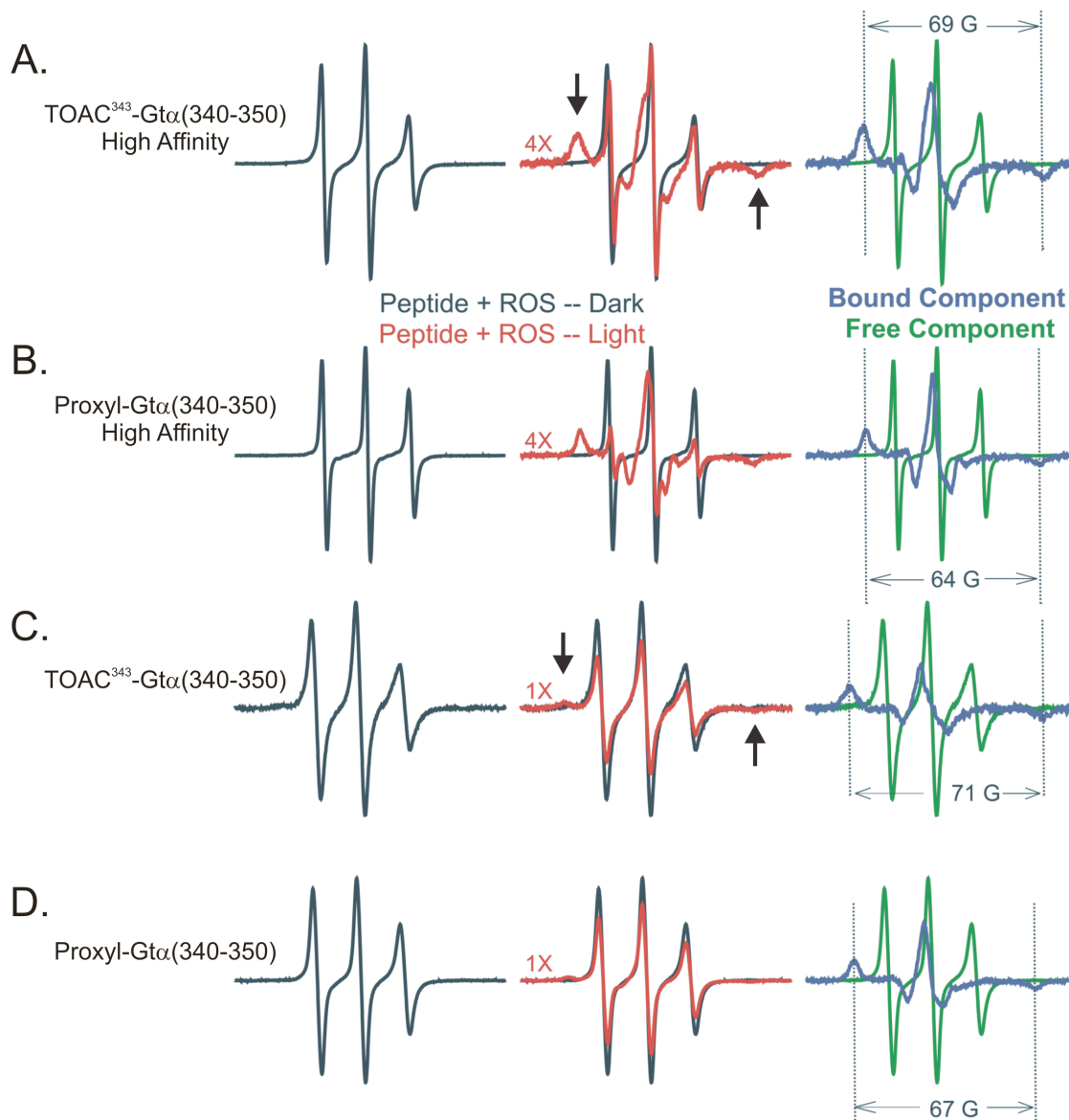


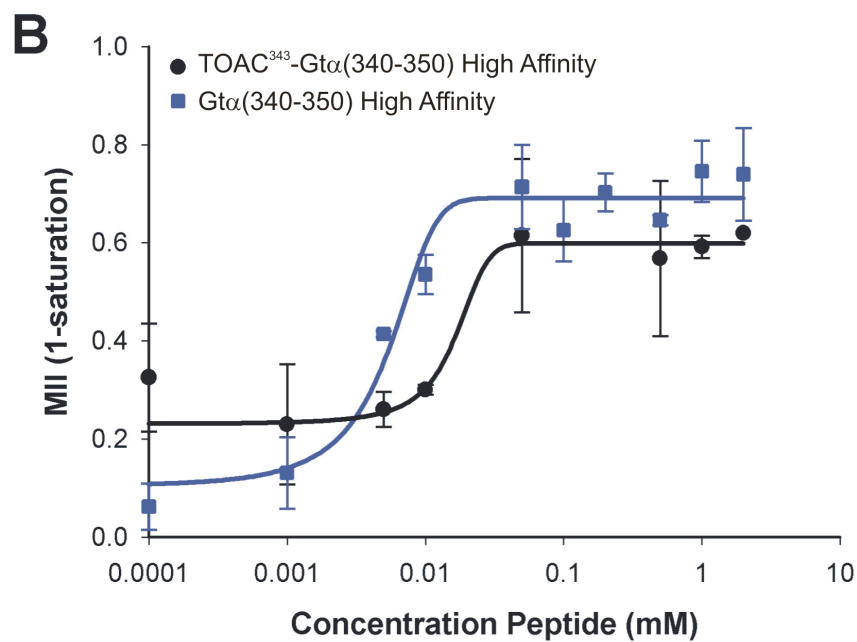
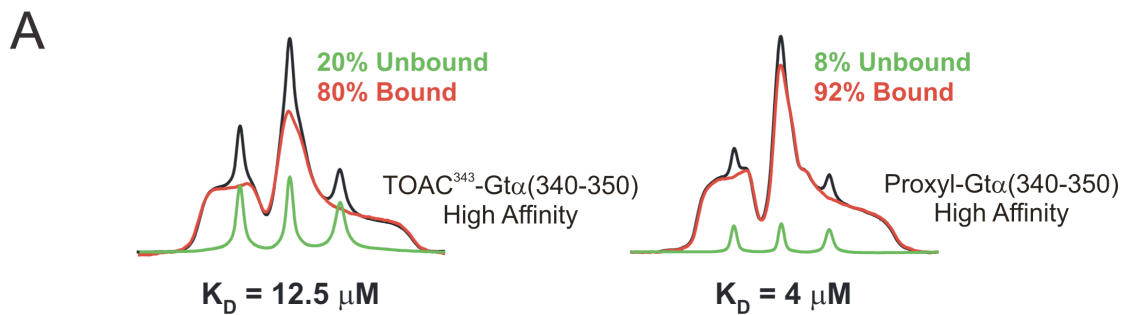
EPR Studies of Functionally Active, Nitroxide Spin- Labeled Peptide Analogs of the C-terminus of a G-Protein Alpha Subunit

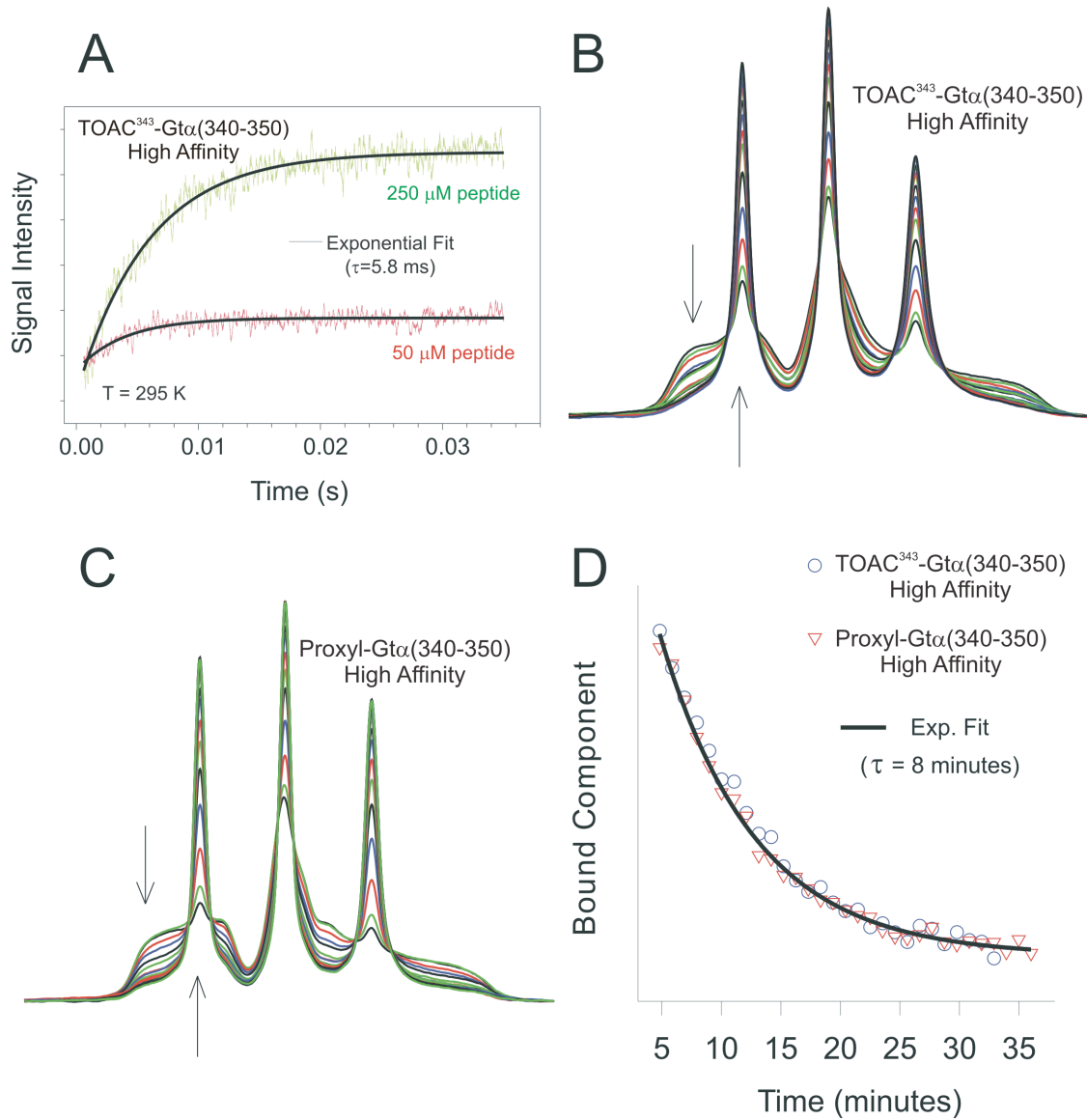
Journal:	<i>Biochemistry</i>
Manuscript ID:	bi-2010-00846c.R1
Manuscript Type:	Article
Date Submitted by the Author:	n/a
Complete List of Authors:	Van Eps, Ned; UCLA, Chemistry & Biochemistry Anderson, Lori; University Nebraska-Lincoln Kisselev, Oleg; Saint Louis University, Ophthalmology Baranski, Thomas; Washington University School of Medicine, Medicine Hubbell, Wayne; UCLA, Chemistry & Biochemistry Marshall, Garland; Washington University Medical School, Center for Computational Biology

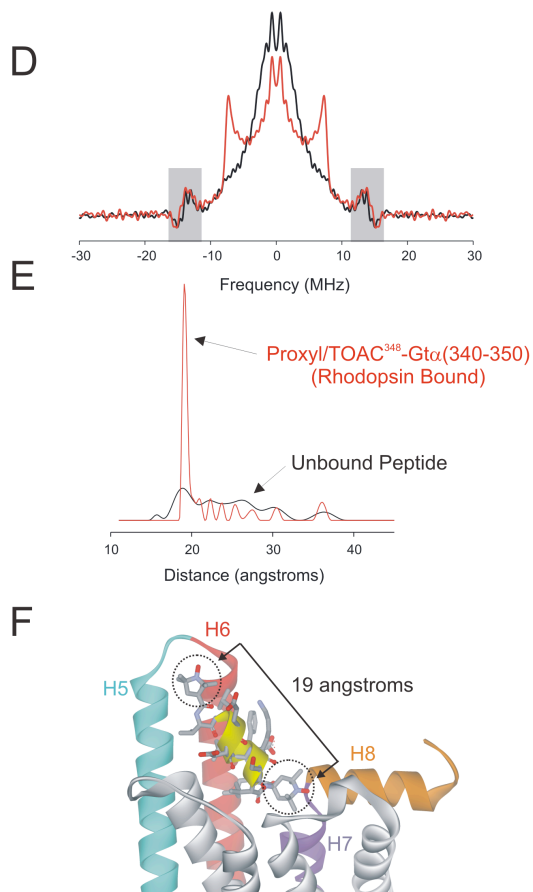
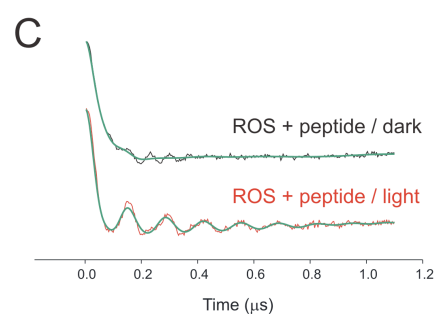
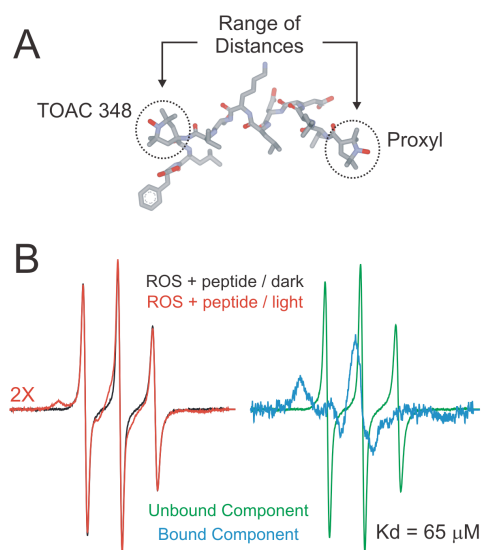












(Submitted to Biochemistry)

EPR Studies of Functionally Active, Nitroxide Spin- Labeled Peptide Analogs of the C-terminus of a G- Protein Alpha Subunit

Ned Van Eps³, Lori L. Anderson^{1,2*}, Oleg G. Kisselev⁴, Thomas J. Baranski², Wayne L.
Hubbell^{3,#} and Garland R. Marshall^{1,#}*

¹Department of Biochemistry and Molecular Biophysics; ²Departments of Medicine, Molecular
Biology and Pharmacology, Washington University, St. Louis, MO 63110

³Jules Stein Eye Institute and Department of Chemistry and Biochemistry, University of
California, Los Angeles, California 90095-7008

⁴Departments of Ophthalmology and of Biochemistry and Molecular Biology, St. Louis
University School of Medicine, St. Louis, MO, 63104

* These authors contributed equally to the work.

Corresponding authors

ABSTRACT

The C-terminal tail of the transducin alpha subunit, Gt α (340-350), is known to bind and stabilize the active conformation of rhodopsin upon photoactivation (R*). Five spin-labeled analogs of Gt α (340-350) demonstrated native-like activity in their ability to bind and stabilize R*. The spin label 2,2,6,6-tetramethylpiperidine-1-oxyl-4-amino-4-carboxylic acid (TOAC) was employed at interior sites within the peptide, whereas a Proxyl (3-carboxyl-2,2,5,5-tetramethylpyrrolidinyloxy) spin label was employed at the amino terminus of the peptide. Upon binding to R*, the electron paramagnetic resonance spectrum of TOAC³⁴³-Gt α (340-350) revealed greater immobilization of the nitroxide when compared to that of the N-terminal modified Proxyl-Gt α (340-350) analog. A double-labeled Proxyl/TOAC³⁴⁸-Gt α (340-350) was examined by DEER spectroscopy to determine the distribution of distances between the two nitroxides in the peptides when in solution and when bound to R*. TOAC and Proxyl spin labels in this GPCR-G-protein α -peptide system provide unique biophysical probes that can be used to explore the structure and conformational changes at the rhodopsin-G-protein interface.

1
2
3 Abbreviations: EPR, electron paramagnetic resonance; TOAC, 2,2,6,6-tetramethylpiperidine-1-
4
5 oxyl-4-amino-4-carboxylic acid; Proxyl, 3-carboxyl-2,2,5,5-tetramethyl-pyrrolidinyloxy, free
6
7 radical; G-protein, heterotrimeric guanine nucleotide binding protein; GPCR, G-protein coupled
8
9 receptor; DEER, double electron-electron resonance
10
11
12
13
14
15
16
17
18
19
20
21
22
23
24
25
26
27
28
29
30
31
32
33
34
35
36
37
38
39
40
41
42
43
44
45
46
47
48
49
50
51
52
53
54
55
56
57
58
59
60

1
2
3
4
5
6 Spin-labeled proteins and peptides, as used in EPR studies, provide a dynamic view of
7
8 biological phenomenon. In site-directed spin labeling (SDSL), nitroxide amino acids are
9
10 selectively introduced into a peptide or protein, and the electron paramagnetic resonance is
11
12 analyzed to provide information on sequence-specific secondary and tertiary structure,
13
14 membrane protein topography and electrostatic potential (1), conformational changes (2), protein
15
16 dynamics (3), and inter-nitroxide distances (4-7). In most studies, the nitroxide side chain
17
18 designated R1 has been employed (Figure 1a). Crystallographic (8-11), mutagenic (12, 13) and
19
20 spectral simulation studies (14) revealed that internal motions of the side chain are constrained
21
22 due to interactions of the disulfide with main-chain atoms. Thus, the dynamics, and hence the
23
24 EPR spectra, are primarily determined by limited torsional oscillations about two dihedral angles
25
26 (angles X_4 and X_5 in Figure 1a). As a result of this constrained motion, the EPR spectrum is
27
28 highly sensitive to additional backbone fluctuations and to modulations of the motion due to
29
30 interactions of the nitroxide with the local environment in the protein. Thus, the EPR spectrum is
31
32 a “fingerprint” of the local structure and dynamics. For this reason, EPR spectral lineshape
33
34 analysis of R1 in proteins has been able to reveal and characterize conformational changes (2),
35
36 in some cases with real time resolution (15-16). Of particular interest for the present report are
37
38 SDSL studies of receptors systems, including the GPCR rhodopsin (17,18) its cognate G protein
39
40 transducin (19-23), and the estrogen receptor alpha (24). In addition to investigating
41
42 conformational changes, EPR spectra of R1 have been analyzed to determine the amplitudes of
43
44 backbone fluctuations on the nanosecond time scale (3). This is of interest because sequences
45
46 with flexibility on this time scale often turn out to be involved in protein-protein recognition.
47
48
49
50
51
52
53
54
55
56
57
58
59
60

1
2
3 One of the most powerful tools for static structure determination in SDSL is inter-spin
4 distance measurement in systems containing two nitroxide side chains. Under normal
5
6 physiological temperatures, inter-spin distances in the range of 10-20 Å can readily be measured
7
8 using continuous wave (CW) EPR deconvolution methods to extract dipolar broadening (4,5). At
9
10 low temperature, the time-domain method DEER (Double Electron Electron Resonance) extends
11
12 the distance range to near 80 Å (6,7). Most importantly, DEER resolves multiple discrete
13
14 distances and their corresponding distributions, with the only disadvantage that time-resolved
15
16 changes in distances are not readily monitored due to the requirement of low temperature. Thus,
17
18 the range of distances between 10 – 80 Å is accessible, ideal for mapping structure and structural
19
20 changes in proteins and complexes.
21
22
23
24
25
26

27 Although the R1 side chain has proven extremely useful as a monitor of local protein
28
29 structure and dynamics, the inherent potential for the R1 side chain to adopt multiple rotamers in
30
31 proteins warrants particular care for interpretation of interspin-distances in terms of protein
32
33 structure. Despite the fact that R1 has a limited conformational space at solvent-exposed sites
34
35 (8-11), interactions with the protein can result in the population of higher energy rotamers. This
36
37 can be mitigated for measuring structural *changes* by judicious selection of sites for R1
38
39 introduction (18), but uncertainty remains for relating inter-nitroxide distances to distances
40
41 between C α carbons. This uncertainty can be overcome to some extent with sufficient distance
42
43 constraints to localize the spatial position of the nitroxide, but practical applications requires
44
45 multiple nitroxide pairs (18).
46
47
48
49

50 The present report explores the utility of a more constrained side chain, TOAC (Figure
51
52 1b). The tetra-substituted α,α -dialkyl spin label TOAC (2,2,6,6-tetramethylpiperidine-1-oxyl-4-
53
54 amino-4-carboxylic acid) (25) contains a nitroxide ring attached to the peptide backbone through
55
56
57
58
59
60

1
2
3
4 its α -carbon (Figure 1b). Due to the self-imposed cyclic constraints of TOAC, it provides a
5
6 useful tool in measuring conformational changes using DEER, since distances between TOACs
7
8 are not compromised by uncertainties in rotamer distribution, but TOAC does have twist-boat
9
10 ring conformers in which the 2p orbital of the nitroxide is inclined at different angles with
11
12 respect to an alpha helix axis (26, 27). The fixed spatial orientations of TOACs can complicate
13
14 simple distance measurements, but this feature is of potential use in measuring relative
15
16 orientations of structural elements in a protein (28).
17
18
19

20 The introduction of TOAC into peptide chemistry allowed the first use of linking a rigid
21
22 spin label to a growing peptide chain through an amide bond. Although incorporation of TOAC
23
24 has become common by chemical synthesis due to its high sensitivity for monitoring
25
26 conformational changes within the peptide scaffold, its use in biologically relevant systems is
27
28 limited, as it cannot be incorporated biosynthetically and is more difficult to synthetically
29
30 incorporate in peptide sequences for chemical ligation due to its lower reactivity due to steric
31
32 hinderance.
33
34
35

36 Acetyl-TOAC- α -MSH (29) and N-terminal TOAC-derivatives of angiotensin (30, 31)
37
38 and bradykinin (31) demonstrated the first syntheses of spin-labeled peptide hormones which
39
40 maintained biological activity. Furthermore, a series of three, TOAC-labeled, neuropeptide Y
41
42 analogs maintained their ability to bind the G-protein coupled receptor Y, demonstrating the
43
44 ability to obtain structural informational upon binding of the NPY ligand to its receptor (32).
45
46 Smythe et al were the first to incorporate two TOAC residues into model helical peptides for
47
48 comparison with EPR studies on the more flexible SDSL label R1 (33, 34).
49
50
51

52 Herein, TOAC-labeled G α -transducin (G α)-terminal peptides are used to probe changes
53
54 in peptide mobility that accompany binding at the GPCR rhodopsin/G-protein interface.
55
56
57
58
59
60

1
2
3 Rhodopsin, the primary visual receptor and the prototype of G-protein-coupled receptors, is one
4 of the best characterized of all GPCRs. Upon photoactivation, rhodopsin forms an active
5 signaling conformation, metarhodopsin II (MII) resulting in interaction with transducin ($G\alpha\beta\gamma$),
6
7
8 its heterotrimeric G-protein partner. Interaction between $G\alpha\beta\gamma$ and MII stabilizes the MII state
9
10 and initiates a signal cascade ultimately leading to nucleotide exchange on $G\alpha$ resulting in
11
12 dissociation of $G\alpha\beta\gamma$ from the GPCR as $G\beta\gamma$ and $G\alpha$ -GTP (35, 36). A synthetic undecapeptide
13
14 corresponding to $G\alpha(340-350)$ (IKENLKDCGLF) binds to activated rhodopsin and stabilizes
15
16 the MII state, thus mimicking the effects of transducin itself (37). The structure of the $G\alpha$ -
17
18 peptide bound to photoactivated rhodopsin was solved using transferred nuclear Overhauser
19
20 effect (TrNOE) NMR spectroscopy (38, 39).
21
22
23
24
25
26
27

28 Results reported by Kisselev *et al.* demonstrated that upon light activation, $G\alpha(340-$
29
30
31
32
33
34
35
36
37
38
39
40
41
42
43
44
45
46
47
48
49
50
51
52
53
54
55
56
57
58
59
60
 $350)$ shifts from a highly disordered conformation to a ordered continuous helix terminated by a
C-terminal capping motif, associated with the formation of a unique clustering of residues,
namely L344, K345, L349 and F350 (39). Similar structural results were obtained by Koenig *et*
al using transferred NOE on an analog of $G\alpha(340-350)$ bound to MII (40) as well as by the
crystal structure of the undecapeptide bound to opsin (41). The conformational changes that
occur in the C-terminal sequence upon receptor interaction were further investigated by
fluorescence and spin labeling of substituted cysteines in the $G\alpha$ subunit (42, 43). Further
understanding these conformational changes should provide better insight into possible
mechanisms of nucleotide exchange of α -subunits of G-proteins.

Here, the syntheses of spin-labeled $G\alpha$ peptide analogs, $TOAC^{343}$ - $G\alpha(340-350)$ and
Proxyl- $G\alpha(340-350)$ and the double-labeled Proxyl/ $TOAC^{348}$ - $G\alpha(340-350)$ are reported. Each
retained the ability to stabilize the MII state of rhodopsin. In addition, the analogous [$TOAC^{343}$]

1
2
3 and Proxyl analogs of the 100-fold higher-affinity peptide (VLEDLKSCGLF) reported from
4 phage display (44) were prepared. Finally, the light-dependent binding of these analogs to native
5 rhodopsin in disk membranes was demonstrated.
6
7
8
9

10 11 12 **MATERIALS AND METHODS**

13 *Peptide Synthesis*

14
15
16 Native Gt α (340-350) IKENLKDCGLF was synthesized in 0.2 mmol scale by manual
17 Fmoc-protection strategy using Fmoc-Phe-Wang resin and the following Fmoc amino acid
18 derivatives: Fmoc-Lys(Boc), Fmoc-Glu(tBu), Fmoc-Asn(Trt), Fmoc-Asp(tBu), and Fmoc-
19 Cys(Trt). Couplings were facilitated by 2-(1H-benzotriazole-1-yl)-1,1,3,3-tetramethyluronium
20 hexafluorophosphate (HBTU) in the presence of DIPEA in DMF, with a 3-fold excess over the
21 amino component. Crude peptide was released from the Wang resin using Reagent K (82.5%
22 trifluoroacetic acid, 5% water, 5% thioanisole, 5% phenol and 2.5% 1,2-ethanedithiol). After
23 reacting for 1 hour, the mixture was filtered, washed with TFA, evaporated and the crude peptide
24 was precipitated with diethyl ether. The peptide was purified by preparative HPLC using a C-18
25 column with a 10-90% gradient (solvent A: 0.5% TFA in H₂O; solvent B: 0.038% TFA/90%
26 acetonitrile/10% H₂O) over 25 minutes. Characterization by MALDI mass spectroscopy gave
27 the expected molecular weight (m/z) of 1279.53.
28
29
30
31
32
33
34
35
36
37
38
39
40
41
42
43
44

45
46 The synthesis of TOAC³⁴³-Gt α (340-350) IKE-TOAC-LKDCGLF and the respective
47 high-affinity analog VLE-TOAC-LKSVGLF followed the same synthesis as above with the
48 following modifications. The stable nitroxide Fmoc-amino acid TOAC was synthesized
49 according to a reported procedure (46). The coupling steps involving the carboxyl and amino
50 groups of TOAC were achieved with 5 eq of Fmoc-amino acid activated by 5 eq of TFFH and 10
51
52
53
54
55
56
57
58
59
60

1
2
3 eq of DIPEA and repeated twice for 2 hours. After incorporation of TOAC and Asp, unreacted
4
5 amino groups were acetylated with acetic anhydride/DMF using a catalytic amount of DMAP for
6
7 30 minutes. The peptide was cleaved from the resin using HF in the presence of 5% anisole.
8
9 Following cleavage, the peptide was precipitated with ether, filtered, and extracted with 30%
10
11 acetic acid and water. The crude peptide was submitted to alkaline treatment (0.02 M
12
13 ammonium acetate, pH 9, 3 h) to recover the paramagnetic moiety. The peptide was purified by
14
15 preparative HPLC using a linear gradient of 10-90% B over 26 minutes with solvent A as 0.05 M
16
17 ammonium acetate, pH 5 and solvent B as 90% acetonitrile. Characterization by electrospray
18
19 ionization mass spectroscopy gave the expected molecular mass of 1363 and 1302 for the low-
20
21 and high-affinity analogs respectively.
22
23
24
25
26

27 Proxyl-Gt α (340-350), its respective high-affinity analog and the double-labeled
28
29 Proxyl/TOAC³⁴⁸-Gt α (340-350) were synthesized through coupling of 3-carboxy-Proxyl (3-
30
31 carboxyl-2,2,5,5-tetramethyl-pyrrolidinyloxy, Aldrich, St. Louis, MO) to the amino terminus of
32
33 the peptide sequences as synthesized above. Activation of the carboxyl group of Proxyl (5 eq)
34
35 was achieved with 5 eq TFFH and 10 eq DIEA and followed by coupling twice for 2 hours.
36
37 Cleavage and purification was the same as for TOAC³⁴³-Gt α (340-350). Analysis by electrospray
38
39 ionization gave the expected molecular mass of 1448 and 1388 for the low- and high-affinity
40
41 analogs and 1531 for the double-labeled peptide, respectively.
42
43
44
45

46 ***Preparation of Rod Outer Segments***

47
48 Urea-washed rod outer segments (ROS) were prepared from dark-adapted retinas (W.L.
49
50 Lawson Co., Lincoln, NE) using a sucrose-gradient procedure as previously described (46). All
51
52 purification steps were carried out in dim red light (Kodak safelight filter, 650 nm cutoff) at 4°C.
53
54
55
56
57
58
59
60

1
2
3 The final ROS samples were resuspended in a 20 mM MES buffer (pH 6.8) containing 100 mM
4 NaCl, 2 mM MgCl₂, and 10% glycerol and stored at -80 degrees Celsius until further use.

8 *UV/visible spectroscopy*

9
10 The binding affinities of Gtα(340-350), TOAC³⁴³-Gtα(340-350) and the double-labeled
11 Proxyl/TOAC³⁴⁸-Gtα(340-350) to rhodopsin in rod outer segments (ROS) were measured using
12 a Meta II stabilization assay (47) by UV/visible spectroscopy. The samples contained 2.5 μM
13 rhodopsin in ROS membranes (48) and peptides in buffer A (20 mM Tris-HCl pH 8.0, 130 mM
14 NaCl, 1 mM MgCl₂, 1 μM EDTA). The samples were kept on ice and prepared under dim red
15 light to avoid premature bleaching of rhodopsin. The absorption spectrum of dark-adapted
16 rhodopsin was taken, illuminated with 490 ± 5 nm light for 20 s, followed by acquisition of the
17 light-activated spectrum, using a Cary50 spectrophotometer (Varian, Palo Alto, CA). The cuvette
18 compartment was maintained at 4° C. The measurements were done in triplicate at varying
19 peptide concentrations from 1 μM to 5 mM. The Meta II stabilization was calculated as ΔA₃₈₀
20 nm - ΔA_{417 nm}, where ΔA is the absorbance change before and after light activation. The data was
21 fit using the equation MII = Baseline + Range * {[peptide] / ([peptide] + EC50)} to obtain EC50
22 values of the peptides. Baseline and Range values were kept constant throughout all
23 determinations at 0.05 and 0.75, respectively.

43 *EPR Measurements*

44
45 EPR measurements were carried out on a Bruker 580 spectrometer at X-band microwave
46 frequencies using a high-sensitivity resonator (HS0118) with an optical port. Spin-labeled
47 peptides were mixed with dark-adapted ROS in 20 mM MES buffer (pH 6.8) containing 100 mM
48 NaCl, 2 mM MgCl₂, and 10% glycerol and loaded into a quartz flat cell. Low-affinity peptide
49 data were recorded at 277 K to slow the disappearance of the rhodopsin bound component (see
50
51
52
53
54
55
56
57
58
59
60

1
2
3 discussion below), while high-affinity peptide data were recorded at 296 K. Spectra were
4 initially recorded under dim red light. Samples were subsequently photobleached with a tungsten
5 lamp (500 nm cutoff filter) for 40 s and an EPR spectrum was recorded.
6
7
8
9

10 Time-resolved EPR photolysis experiments were initiated with a ~6 ns laser pulse (500
11 nm) from a Q-switched Nd:YAG laser coupled with a tunable optical paramagnetic oscillator
12 (Vibrant, Opotek, Inc., Carlsbad, CA). The magnetic field position was set at the center field
13 trough of the unbound peptide spectrum, and the resulting EPR transient was detected with
14 100kHz field modulation. The signals were recorded with a LeCroy digital oscilloscope (LeCroy
15 Corp., Chestnut Ridge, NY).
16
17
18
19
20
21
22
23

24 **Double Electron Electron Resonance Experiments (DEER)**

25
26
27 Double spin-labeled peptides were mixed with dark-adapted ROS (both in 10% (v/v)
28 glycerol) and flash frozen in the dark in 1.5 mm x 1.8 mm quartz capillaries in liquid nitrogen.
29 DEER measurements were performed at 50 K on a Bruker Elexsys 580 spectrometer with a 2-
30 mm split-ring resonator. Four-pulsed DEER was carried out as previously described (7, 49) with
31 the π pump pulse (16 ns) positioned at the absorption maximum of the field swept spectrum. The
32 observer π (16 ns) and $\pi/2$ (8 ns) pulses were positioned at the low-field line of the spectrum (Δf
33 = 70 MHz). After dark-state data were acquired, the samples were thawed, illuminated with light
34 (500-nm-cutoff filter) and refrozen in liquid nitrogen for a second DEER experiment. All DEER
35 data were analyzed with the DEER Analysis 2009 software package freely available at the
36 website <http://www.epr.ethz.ch/>. Tikhonov regularization and distance distribution widths were
37 optimized using L-curve analysis implemented in the software package.
38
39
40
41
42
43
44
45
46
47
48
49
50
51
52
53
54
55
56
57
58
59
60

RESULTS

Peptide Synthesis

It has been demonstrated that positions that accept Aib (α -aminobutyric acid), will usually also accept TOAC substitutions. Molecular modeling of conformationally constrained peptides identified the analog of Gt α (340-350), AibKAibAibLKDCGLG, that was synthesized and shown to maintain full activity in stabilization of the MII state of rhodopsin (50). Given that Aib mimics the conformational effect of TOAC substitutions on the peptide backbone (51-54), these results suggested that residues I340, E342 and N343 are capable of tolerating substitution. For the work outlined here, we chose substitution with TOAC at N343. A TOAC scan of the C-terminal tail also revealed that substitution of Gly348 with TOAC maintained the ability to stabilize the MII state of rhodopsin (data not shown) and double-labeled Gt α (340-350) Proxyl/TOAC³⁴⁸-Gt α (340-350) was therefore prepared.

Binding of spin-labeled G α peptides to light-activated rhodopsin

EPR studies have focused on characterizing the TOAC³⁴³-Gt α (340-350) (IKE-TOAC-LKDCGLF; Fig. 1D bottom) and the corresponding high-affinity TOAC³⁴³ analog (VLE-TOAC-LKSVGLF) in terms of mobility both in the rhodopsin-bound and unbound forms. Characterization of Proxyl³⁴⁰-Gt α (340-350) (Figure 1D top) and the corresponding high-affinity analog has also been carried out for comparison with the TOAC analogs. The EPR spectra of the spin-labeled peptides in the presence of dark- and light-activated ROS membranes are shown in Figure 2. In each case, the spectrum of the peptide in the presence of ROS membranes in the dark is the same as that for the peptide in buffer, and consists of a single component of three

1
2
3 relatively sharp lines, characteristic of a rapidly and isotropically tumbling nitroxide (Figure 2,
4 left-hand panel). On the other hand, spectra of the peptides in the presence of photoactivated
5 ROS membranes are a composite of two distinct components (Figure 2, center panel), one of
6 which corresponds to the free peptide in solution. The other component is identified by well-
7 resolved hyperfine extrema (arrows, Figure 2) indicative of peptide immobilization and
8 rhodopsin binding. As expected, the amplitude of the bound component is much greater for the
9 high-affinity analogs. The individual components, resolved by spectral subtraction, are shown
10 for each peptide in the right-hand panel of Figure 2. The components corresponding to the
11 bound states (right panel, blue traces) each have line shapes characteristic of highly immobilized
12 nitroxides. A comparison of the spectral components corresponding to the bound states reveals
13 different mobilities for the TOAC and Proxyl analogs. An approximate rotational correlation
14 time (τ_c) for a nitroxide may be computed from the separation of the outer hyperfine extrema
15 ($2A_{zz}$) and that for the same sample in a frozen state in the absence of motion ($2A_{zz}^0$) (55). For
16 the TOAC and Proxyl analogs of the high-affinity peptide bound to photoactivated rhodopsin,
17 $2A_{zz}$ is 69 and 64 Gauss, respectively (Figure 2). For both analogs bound to photoactivated
18 rhodopsin, $2A_{zz}^0$ obtained at 223° K is 74 G (spectra not shown), indicating that the nitroxides
19 in each case are located in a polar environment, presumably facing the solvent. From these
20 values, assuming Brownian motion, τ_c is estimated to be 19.4 and 8.7 ns for the TOAC and
21 Proxyl analogs, respectively. Thus, the TOAC analog of the high-affinity peptide is more
22 immobilized than the corresponding Proxyl analog. Because the rotational diffusion of rhodopsin
23 in the disc is very slow ($\tau_R \approx 12\mu\text{s}$, (56)), and because TOAC is rigidly attached to the peptide
24 backbone, the 19.4 ns correlation time for the TOAC analog directly measures the fluctuation
25
26
27
28
29
30
31
32
33
34
35
36
37
38
39
40
41
42
43
44
45
46
47
48
49
50
51
52
53
54
55
56
57
58
59
60

1
2
3 frequency of the peptide in the rhodopsin binding site. Differences in 2Azz, and hence mobility
4
5 are observed between TOAC and Proxyl in both the low- affinity and high-affinity peptides.
6
7
8
9
10

11 12 *Activity of the Peptides: Stabilization of MII*

13
14
15 The binding of a C-terminal G-alpha peptide or analog to photoactivated rhodopsin can
16
17 be monitored by an increase in the amount of MII due to the presence of the peptide. A dose-
18
19 response curve of concentration of peptide relative to its effect on MII stabilization can be fit to
20
21 the model described in Methods to provide a value for the apparent dissociation constant (Kd).
22
23 Results are compared for the native Gt α (340-350), the TOAC³⁴³-Gt α (340-350) and Proxyl-
24
25 Gt α (340-350) in Figure 1E. The data reveal that the presence of the TOAC³⁴³ or the Proxyl
26
27 groups has little effect on the binding affinity to the receptor. Figure 3B shows examples for the
28
29 TOAC³⁴³-Gt α (340-350) high-affinity peptide compared with the high-affinity peptide without
30
31 TOAC. The fits to the data, shown by the solid traces, give Kd values of 10 μ M and 4.2 μ M,
32
33 respectively. Thus, the presence of the TOAC spin label at 343 increases the Kd by about a
34
35 factor of ≈ 2.5 , corresponding to a modest increase in the free energy of the bound state by 0.5
36
37 kCal/mole due to the TOAC.
38
39
40
41
42
43

44 It is of interest to compare the apparent dissociation constant for a spin-labeled peptide
45
46 determined by the MII stabilization assay with that determined from direct binding using EPR.
47
48 Figure 3A, left-hand panel, shows the absorption EPR spectrum (obtained by integration of the
49
50 first derivative spectra) corresponding to the equilibrium of TOAC³⁴³-Gt α (340-350) high-affinity
51
52 peptide with photoactivated rhodopsin (black trace). Also shown are the individual components
53
54 corresponding to the bound and free peptide (red and green traces, respectively), obtained by
55
56
57
58
59
60

1
2
3 subtraction. Integration of the individual spectra provides the relative equilibrium concentrations
4
5 of each, which gives a K_d of 12.5 μM for the $\text{TOAC}^{343}\text{-Gt}\alpha(340\text{-}350)$ high-affinity peptide. This
6
7 compares favorably with the value of 10 μM obtained from the MII stabilization data shown in
8
9 Figure 3B. Figure 3A, right-hand panel, shows similar data for Proxyl-Gt $\alpha(340\text{-}350)$ high-
10
11 affinity peptide, giving a K_d of 4 μM . This value is essentially identical to that obtained for the
12
13 non-labeled high-affinity analog using the MII stabilization assay, suggesting that the terminal
14
15 location of the spin label does not perturb the peptide-R* interaction. Interestingly, the peptide
16
17 dissociation constants measured in Figure 3A via EPR techniques did not vary over a pH range
18
19 of 6-8 (data not shown).
20
21
22
23
24
25
26

27 *Kinetics of binding for G α peptide analogs*

28
29
30 The kinetics of binding to photoactivated rhodopsin (R*) for the $\text{TOAC}^{343}\text{-Gt}\alpha(340\text{-}350)$
31
32 high-affinity peptide was determined by monitoring the EPR signal after a ~6 ns actinic flash at
33
34 500 nm. Figure 4A shows the EPR spectral amplitude collected at three different peptide
35
36 concentrations (gray, green, and red traces) monitored at the centerfield trough of the EPR
37
38 spectrum, corresponding to the unbound peptide (see Figure 2A, right panel). Data was collected
39
40 as a function of time after the laser pulse and was fit to a single exponential rise (black line) with
41
42 an apparent lifetime of ~6 ms. The time course of peptide binding was independent of the
43
44 peptide concentration for the three concentrations tested, suggesting that the binding event is rate
45
46 limited by structural changes within the rhodopsin photoreceptor that lead to opening of the
47
48 binding site rather than diffusion of the peptide to the receptor. The data were collected under
49
50 either pseudo-first order (2.5 mM peptide) or second order (50 and 250 μM peptide) conditions.
51
52
53
54
55
56
57
58
59
60
61
62
63
64
65
66
67
68
69
70
71
72
73
74
75
76
77
78
79
80
81
82
83
84
85
86
87
88
89
90
91
92
93
94
95
96
97
98
99
100
101
102
103
104
105
106
107
108
109
110
111
112
113
114
115
116
117
118
119
120
121
122
123
124
125
126
127
128
129
130
131
132
133
134
135
136
137
138
139
140
141
142
143
144
145
146
147
148
149
150
151
152
153
154
155
156
157
158
159
160
161
162
163
164
165
166
167
168
169
170
171
172
173
174
175
176
177
178
179
180
181
182
183
184
185
186
187
188
189
190
191
192
193
194
195
196
197
198
199
200
201
202
203
204
205
206
207
208
209
210
211
212
213
214
215
216
217
218
219
220
221
222
223
224
225
226
227
228
229
230
231
232
233
234
235
236
237
238
239
240
241
242
243
244
245
246
247
248
249
250
251
252
253
254
255
256
257
258
259
260
261
262
263
264
265
266
267
268
269
270
271
272
273
274
275
276
277
278
279
280
281
282
283
284
285
286
287
288
289
290
291
292
293
294
295
296
297
298
299
300
301
302
303
304
305
306
307
308
309
310
311
312
313
314
315
316
317
318
319
320
321
322
323
324
325
326
327
328
329
330
331
332
333
334
335
336
337
338
339
340
341
342
343
344
345
346
347
348
349
350
351
352
353
354
355
356
357
358
359
360
361
362
363
364
365
366
367
368
369
370
371
372
373
374
375
376
377
378
379
380
381
382
383
384
385
386
387
388
389
390
391
392
393
394
395
396
397
398
399
400
401
402
403
404
405
406
407
408
409
410
411
412
413
414
415
416
417
418
419
420
421
422
423
424
425
426
427
428
429
430
431
432
433
434
435
436
437
438
439
440
441
442
443
444
445
446
447
448
449
450
451
452
453
454
455
456
457
458
459
460
461
462
463
464
465
466
467
468
469
470
471
472
473
474
475
476
477
478
479
480
481
482
483
484
485
486
487
488
489
490
491
492
493
494
495
496
497
498
499
500
501
502
503
504
505
506
507
508
509
510
511
512
513
514
515
516
517
518
519
520
521
522
523
524
525
526
527
528
529
530
531
532
533
534
535
536
537
538
539
540
541
542
543
544
545
546
547
548
549
550
551
552
553
554
555
556
557
558
559
560
561
562
563
564
565
566
567
568
569
570
571
572
573
574
575
576
577
578
579
580
581
582
583
584
585
586
587
588
589
590
591
592
593
594
595
596
597
598
599
600
601
602
603
604
605
606
607
608
609
610
611
612
613
614
615
616
617
618
619
620
621
622
623
624
625
626
627
628
629
630
631
632
633
634
635
636
637
638
639
640
641
642
643
644
645
646
647
648
649
650
651
652
653
654
655
656
657
658
659
660
661
662
663
664
665
666
667
668
669
670
671
672
673
674
675
676
677
678
679
680
681
682
683
684
685
686
687
688
689
690
691
692
693
694
695
696
697
698
699
700
701
702
703
704
705
706
707
708
709
710
711
712
713
714
715
716
717
718
719
720
721
722
723
724
725
726
727
728
729
730
731
732
733
734
735
736
737
738
739
740
741
742
743
744
745
746
747
748
749
750
751
752
753
754
755
756
757
758
759
760
761
762
763
764
765
766
767
768
769
770
771
772
773
774
775
776
777
778
779
780
781
782
783
784
785
786
787
788
789
790
791
792
793
794
795
796
797
798
799
800
801
802
803
804
805
806
807
808
809
810
811
812
813
814
815
816
817
818
819
820
821
822
823
824
825
826
827
828
829
830
831
832
833
834
835
836
837
838
839
840
841
842
843
844
845
846
847
848
849
850
851
852
853
854
855
856
857
858
859
860
861
862
863
864
865
866
867
868
869
870
871
872
873
874
875
876
877
878
879
880
881
882
883
884
885
886
887
888
889
890
891
892
893
894
895
896
897
898
899
900
901
902
903
904
905
906
907
908
909
910
911
912
913
914
915
916
917
918
919
920
921
922
923
924
925
926
927
928
929
930
931
932
933
934
935
936
937
938
939
940
941
942
943
944
945
946
947
948
949
950
951
952
953
954
955
956
957
958
959
960
961
962
963
964
965
966
967
968
969
970
971
972
973
974
975
976
977
978
979
980
981
982
983
984
985
986
987
988
989
990
991
992
993
994
995
996
997
998
999
1000

1
2
3 coupled to the unimolecular appearance of the active receptor state. Figure 4B shows EPR
4 absorption spectra collected as a function of time after the initial rapid-binding event. As is
5 evident, the broad spectral component, corresponding to the bound peptide, decreases in time
6 with a concomitant increase in the sharp component, reflecting a slow, spontaneous, dissociation
7 of the bound peptide from R*. The decay of the bound signal can be fit with a single exponential
8 with half-life of 8 minutes (Figure 4D, open circles), similar to that for MII decay in native disk
9 membranes (57).

10
11
12
13
14
15
16
17
18
19
20 Similar results were obtained for the dissociation of the Proxyl-Gt α (340-350) high-
21 affinity peptide from R* (Figure 4C), and the data are included in the plot of Figure 4D
22 (triangles). These results further demonstrate the functionality of the spin-labeled Gt α (340-350)
23 analogs in their ability to bind and stabilize R* and to sense the activated conformational state of
24 the receptor.
25
26
27
28
29
30

31 *DEER spectroscopy*

32
33
34 To investigate the conformation of the peptide bound to MII, the high affinity analog of
35 double-labeled Proxyl/TOAC³⁴⁸-Gt α (340-350) (Figure 5A) was prepared so that the distribution
36 of inter-spin distances in the peptide (in solution or when bound to R*) could be monitored by
37 DEER spectroscopy. The K_d of this peptide was 65 μ M, and, as expected the EPR spectra of the
38 unbound and bound peptides reflected rapid isotropic motion and strong immobilization,
39 respectively, similar to the spectra of the peptides containing a single nitroxide (Figure 5B). The
40 featureless dipolar evolution function of the peptide in the presence of dark rhodopsin (Figure
41 5C, upper trace) and the corresponding dipolar spectrum (Figure 5D, black trace) reflect a broad
42 distribution of inter-nitroxide distances in the range 18 to 34 Å, (Figure 5E, black trace),
43 consistent with an ensemble of conformations for the unbound peptide. Distance distributions of
44
45
46
47
48
49
50
51
52
53
54
55
56
57
58
59
60

1
2
3 peaks longer than 34 Å in Figure 5E are inaccurately determined due to the 1.1 μs length of the
4
5 dipolar evolution functions. On the other hand, in the presence of R* striking oscillations are
6
7 evident in the dipolar evolution function (Figure 5C, lower trace) corresponding to a remarkably
8
9 narrow interspin distance distribution centered at 19 Å (Figure 5E, red trace). Modeling of the
10
11 nitroxides in the crystal structure conformation of the peptide (41) (Figure 5F) shows this
12
13 distance to be consistent with the crystal structure and the unique configuration of the R*-bound
14
15 G_{tα}(340-350) as determined by Kisselev et al. from NMR (39).
16
17
18
19
20
21

22 DISCUSSION

23
24 Heterotrimeric α-subunits have been shown to have several contact regions that are
25
26 critical for receptor interaction (19, 58). One of these regions is apparently the C-terminal
27
28 sequence of G_{tα}, as shown by the fact that a synthetic undecapeptide corresponding to G_{tα}(340-
29
30 350) binds to R* and stabilizes the MII state, thus mimicking the effects of transducin itself (37).
31
32
33

34
35 In this study, we provide evidence that five spin-labeled G_{tα}(340-350) analogs maintain
36
37 their ability to bind and stabilize the photoactivated MII state of rhodopsin. Receptor binding
38
39 was detected by immobilization of incorporated TOAC and Proxyl residues as the peptide adopts
40
41 a highly restricted bound conformation. Comparison between the peptide analogs revealed a
42
43 higher degree of immobilization with the TOAC compared to the Proxyl analog. The difference
44
45 in immobilization can be explained in part by the fact that the N-terminal Proxyl label is
46
47 connected by an amide linkage to the G_{tα}(340-350) backbone, and thus potentially has two
48
49 additional rotational degrees of freedom relative to TOAC. TOAC is incorporated directly within
50
51 the peptide chain and has only limited internal motion relative to the backbone. Hence, when the
52
53 peptide is immobilized on R*, so is the TOAC nitroxide. Interestingly, however, there is some
54
55
56
57
58
59
60

1
2
3 degree of motion on the ns time scale still present in the bound TOAC³⁴³-Gtα(340-350) and
4
5 high-affinity analog that cannot be attributed to R* rotational diffusion. The rotational
6
7 correlation time of rhodopsin in native disk membranes has been measured to be 20-40 μs (59,
8
9 60). This motion is too slow to affect the EPR lineshape, which is sensitive to motion in the 100
10
11 ps – 100 ns time domain. Thus, the ns motions detected in the bound peptide reflect structural
12
13 fluctuations of the peptide in the binding site on this time scale. It should be possible to construct
14
15 approximate partition functions from the distance distributions seen in Figure 5 to estimate the
16
17 change in entropy of the peptide ligand on binding to photoactivated rhodopsin.
18
19
20
21

22
23 Consistent with the bound conformation of Gtα(340-350) peptides to R* observed by
24
25 NMR is the crystal structure of the complex of opsin with this undecapeptide (41). The crystal
26
27 structure helps to further rationalize the differences in nitroxide rotational correlation times of
28
29 the Proxyl and TOAC adducts (see discussion above). Models of the Proxyl peptide using the
30
31 crystallographic data show that this label projects outward toward solvent (see Figure 5F).
32
33 Motion due to the additional rotational degrees of freedom is consistent with the higher mobility
34
35 of the Proxyl relative to the TOAC nitroxide. Note, however, that the Proxyl is still quite
36
37 immobilized, presumably due to contacts of the nitroxide ring with nearby side chains in
38
39 rhodopsin. The TOAC³⁴³-Gtα(340-350) peptide is also solvent accessible (model not shown),
40
41 but the internal constraints of this spin label prevent additional nitroxide motion. Finally, a
42
43 TOAC label placed at position 348 reduced the affinity of the labeled peptide (see Figure 5B),
44
45 likely because the TOAC-348 residue is predicted to have steric clashes with the receptor near
46
47 the helix 7/8 region (see Figure 5F).
48
49
50
51
52

53
54 Studies of peptide binding kinetics to a cognate receptor are an important strategy
55
56 to explore the mechanism of protein-protein recognition. The kinetics of binding of Gtα(340-
57
58
59
60

1
2
3 350) and the high-affinity analog to R* have been previously investigated at low temperature
4
5 (1.5 deg C) and high pH (7.9) by monitoring the production of “extra MII” induced by peptide
6
7 binding (61). An advantage of the EPR method described here is that it is a direct measure of the
8
9 binding interaction compared to the extra MetaII assay which relies upon changes in
10
11 chromophore protonation states at a receptor site distant from the receptor/G-protein interface. In
12
13 addition, physiological temperatures, a wide range of pH values and high concentrations of
14
15 native disc membranes can be used in the EPR method to investigate the binding mechanism.
16
17 The latter point is raised because light scattering artifacts due to high concentration of membrane
18
19 vesicles can complicate interpretation of optical signals, but present no problem in magnetic
20
21 resonance detection. Light scattering methods have also been used to measure peptide binding to
22
23 R*, but this method requires an increase in mass of the peptide, accomplished by fusing the
24
25 peptide to maltose binding protein (MBP, 42.5 kD) (62). While these fused peptides were shown
26
27 to bind to rhodopsin in a light-dependent manner, rate data were likely influenced by the
28
29 presence of MBP due to changes in diffusion constant and, most importantly, to steric constraints
30
31 on the binding event. It could be argued that the presence of the spin label in the peptide could
32
33 also modify the binding kinetics, but the similarity of the Kd for the singly labeled and native
34
35 peptides suggest otherwise.
36
37
38
39
40
41
42

43
44 As shown by the data in Fig. 4, the rate of peptide binding to R* as measured by EPR
45
46 follows a single exponential time course that is apparently rate limited by conformational
47
48 changes in rhodopsin that lead to the binding competent state of the receptor. This is consistent
49
50 with earlier studies which showed fast proton release within rhodopsin upon formation of the
51
52 peptide/receptor complex (16) in DM micelles. The proton release was rate limited by the
53
54 appearance of the active receptor state at much lower reagent concentrations than used in the
55
56
57
58
59
60

1
2
3 current work verifying the validity of the rate limiting step approximation. The time constant
4 for binding to rhodopsin in ROS membranes observed here (≈ 6 ms) is in the time window for
5 formation of deprotonated forms of the receptor detected optically at 380nm (MIIa, MIIb,
6 MIIbH⁺) (63-65); presumably the binding competent state corresponds to one of these
7 intermediates. SDSL data first provided direct evidence that the outward movement of
8 transmembrane helix 6 (TM6) by about 5 Å gives rise to the activated state of the receptor (18,
9 66). The outward movement of TM6 is consistent with generation of a binding pocket for the C-
10 terminal tail of the G α subunit (and the corresponding peptides) within the intracellular loops of
11 R*. This model is directly supported by the recent crystal structure of an opsin/G α (340-350)
12 peptide (41). It is thus reasonable to speculate that the peptide binding is rate-limited by the
13 movement of TM6. The time constant for TM6 movement following an activating light flash has
14 in fact been measured by SDSL to be ≈ 2 ms, and was shown to correspond to the formation of
15 MIIb, but this was determined for rhodopsin in micelles of DM where rate constants for
16 interconversion of the intermediates are generally accelerated (16). Future studies will be
17 required to identify the specific intermediate competent for peptide binding in the native
18 membrane.

19
20
21
22
23
24
25
26
27
28
29
30
31
32
33
34
35
36
37
38
39
40
41 The ability to synthesize fully active, TOAC-labeled analogs of G α (340-350) provides a
42 strategy for mapping the structure of the rhodopsin-peptide complex using distance
43 measurements between pairs of spins, one in the peptide and the other at selected sites
44 throughout the cytoplasmic domain of rhodopsin. Such measurements will determine the relative
45 orientation and position of the bound peptide within the complex, and may identify any
46 additional binding modes of lower affinity. The TOAC spin label is ideally suited for this
47 purpose, because incorporation of α , β , and γ carbons as well as the nitroxide moiety into one
48
49
50
51
52
53
54
55
56
57
58
59
60

1
2
3 heterocyclic structure eliminates rotation about side-chain bonds, effectively fixing the nitroxide
4 relative to the backbone. This is a significant advantage over the more commonly used nitroxide
5 side chains where the possible existence of multiple rotamers complicates the interpretation of
6 interspin distances.
7
8
9
10
11

12
13 Incorporation of synthetic peptides into a $G\alpha$ subunit by expressed protein ligation has
14 been demonstrated (67, 68), setting the stage for future studies that incorporate a TOAC-labeled
15 $G\alpha(340-350)$ peptide into the full-length $G\alpha$. Thus, it would be possible to compare salient
16 structural features of the complex formed with R^* by the isolated peptide with that formed by the
17 full-length $G\alpha$. Such studies using the internally constrained TOAC should be able to measure
18 structural heterogeneity at the rhodopsin/transducin interface and explore the effect of allosteric
19 regulators. Such studies should provide insight into enzymatic mechanisms of transducin
20 activation by R^* .
21
22
23
24
25
26
27
28
29
30
31
32
33
34
35
36

37 **Acknowledgements:** This research was supported in part by grants from the Lucille P. Markey
38 Predoctoral Fellowship (to L.L.A.), the Chemistry Biology Interface Pathway T32GM0878 (to
39 L.L.A.); NIH grants GM68460, GM53630, and EY1211301 (to G.R.M.), GM71634 and
40 GM63720 (to T.J.B.), GM63203, EY18107 and RPB (to O.G.K.), EY05216 (to W.L.H.), and the
41 Jules Stein Professorship endowment.
42
43
44
45
46
47
48
49
50
51
52

53 **FIGURE LEGENDS**

54
55
56
57
58
59
60

1
2
3 **Figure 1. Chemical structures of spin-labels and peptides and the binding of peptides to**
4 **activated rhodopsin.** A. Spin label R1 (cysteine(*S*-(2,2,5,5-tetramethyl-2,5-dihydro-1H-pyrrol-
5 3-yl)methyl-disulfide) used in SDSL with potential degrees of freedom indicated (X_1 - X_5
6 dihedrals). B. TOAC (2,2,6,6-tetramethyl-piperadine-1-oxyl-4-amino-4-carboxyl) spin labels. C.
7 Proxyl (2,2,5,5-Tetramethyl-3-carboxyl-pyrrolidine-1-oxyl) spin label used to modify the amino
8 terminus. D. Chemical structures of two spin-labeled peptides. E. MII stabilization assay for
9 native $G_{t\alpha}(340-350)$ compared with Proxyl- $G_{t\alpha}(340-350)$ and TOAC³⁴³- $G_{t\alpha}(340-350)$.
10
11
12
13
14
15
16
17
18
19
20
21

22 **Figure 2. EPR spectra of the indicated spin-labeled peptides.** Left hand panel: spectra in the
23 presence of dark-adapted ROS membranes; Center panel: spectra in the presence of
24 photoactivated ROS membranes (red trace) compared to those in the dark-adapted state (black
25 trace); right-hand panel: spectra of the pure bound (blue trace) and unbound (green trace) states
26 obtained by spectral subtraction. The high-affinity peptide data was recorded with 2G
27 modulation amplitude at a temperature of 296° K. The low-affinity TOAC³⁴³- $G_{t\alpha}(340-350)$ and
28 $G_{t\alpha}(340-350)$ Proxyl- $G_{t\alpha}(340-350)$ peptide data was recorded with a 4G modulation amplitude
29 and a temperature of 277° K to facilitate detection of the bound component. The higher
30 modulation accounts for the broader lines in the spectra of the unbound component in (C) and
31 (D). EPR spectra in the left-hand and center panels have been normalized to the same number of
32 spins, and plotted with the indicated scaling factor. Individual component spectra (right-hand
33 panel) are arbitrarily scaled for direct line-shape comparison. The samples were in 20 mM MES
34 buffer (pH 6.8) containing 100 mM NaCl, 2 mM MgCl₂, and 10% glycerol.
35
36
37
38
39
40
41
42
43
44
45
46
47
48
49
50
51
52
53
54
55
56
57
58
59
60

Figure 3. Binding of the high-affinity spin-labeled peptides to photoactivated rhodopsin.

(A) Absorption EPR spectra for the TOAC and Proxyl high-affinity peptides in equilibrium with photoactivated rhodopsin at 296° K. The composite absorption spectra (black lines) are shown with the individual spectral components overlaid in green and red. The percentage of rhodopsin-bound peptide was determined by spectral integration. The concentration of rhodopsin and spin-labeled peptide were 90 and 50 μM respectively. The samples were in 20 mM MES buffer (pH 6.8) containing 100 mM NaCl, 2 mM MgCl_2 , and 10% glycerol. B. Dose-responses of MII formation to determine K_d s for TOAC³⁴³-Gt α (340-350) and Gt α (340-350) high-affinity peptides. The measurements were made independently with different preparation of ROS and the graphs were not normalized to overlap initial and final values.

Figure 4. Binding and dissociation kinetics for high-affinity spin-labeled peptides. A)

Transient EPR changes for the TOAC³⁴³-Gt α (340-350) high-affinity peptide collected at the centerfield trough of the free peptide spectrum are plotted as a function of time after the laser flash. The gray, green, and red traces were collected at peptide concentrations of 2.5 mM, 250 and 50 μM , respectively. The rhodopsin concentration was 250 μM . The samples were in 20 mM MES buffer (pH 6.8) containing 100 mM NaCl, 2 mM MgCl_2 , and 10% glycerol. All three traces were well fit with a single exponential function with a lifetime of 5.8 ms (black solid lines). B) EPR absorption spectra as a function of time following the rapid transient showing the decay of the immobile spectral component and the appearance of a mobile species for the TOAC³⁴³-Gt α (340-350) high-affinity peptide and C, for Proxyl-Gt α (340-350) high-affinity peptides. The arrows indicate the direction of the line-shape changes in time. D) Decay of the bound component with time; blue circles, TOAC³⁴³-Gt α (340-350) high-affinity peptides; red triangles,

1
2
3 Gt α (340-350) Proxyl-Gt α (340-350) high-affinity peptides. A single exponential (black line) of
4
5 time constant 8 min was fit to the data.
6
7
8
9

10 **Figure 5. DEER distance measurements for the double spin-labeled peptide**

11 **Proxyl/TOAC³⁴⁸-Gt α (340-350).** A) Diagram of the high affinity double-labeled undecapeptide.

12
13
14
15 A range of distances between spin labels was anticipated in the unbound peptide in solution; B)

16
17
18 Estimation of the dissociation constant of the peptide. EPR spectrum of 90 μ M ROS mixed with

19
20
21 50 μ M peptide before (black trace) and after (red trace) photobleaching. The individual spectral

22
23
24 components were obtained as above, and a K_d of 65 μ M was determined. The samples were in

25
26
27 20 mM MES buffer (pH 6.8) containing 100 mM NaCl, 2 mM MgCl₂, and 10% glycerol. C)

28
29
30 Dipolar evolutions functions for the unbound (black trace) and rhodopsin bound (red trace)

31
32
33 peptide. The ROS and peptide concentrations were 250 and 200 μ M, respectively. The green

34
35
36 traces represent fits to the data using Tikhonov regularization as implemented in the DEER

37
38
39 Analysis 2009 software package (see Methods). The high frequency oscillations observed in the

40
41
42 unbound peptide dipolar evolution function are electron/proton ESEEM signals that are not fit

43
44
45 using the DEER Analysis software package. D) Dipolar spectra of the unbound (black trace)

46
47
48 and rhodopsin-bound (red trace) peptide. The gray highlighted regions indicate frequencies

49
50
51 where ESEEM signals appear. E) Distance distributions for the unbound (black trace) and

52
53
54 rhodopsin-bound (red trace) peptide, and F) Model of the rhodopsin bound double-labeled

55
56
57 Proxyl/TOAC³⁴⁸-Gt α (340-350) high-affinity peptide based on the peptide-bound crystal

58
59
60 structure of opsin (39). Helix 5, 6, 7, and 8 in opsin are colored cyan, red, purple, and orange

respectively. The peptide ribbon is shown in yellow while side chains are shown as sticks. The

distance as measured by DEER between the two spin labels matched that predicted from NMR

1
2
3 structural data (model not shown) as well as the peptide-bound crystal structure of opsin (39).
4
5 The Proxyl side chain is more solvent exposed and is projected toward the helix 5/6 loop in
6
7 opsin, while TOAC-348 is buried near the helix 7/8 interface. Steric contacts between TOAC-
8
9 348 and opsin likely reduce its binding affinity relative to other spin-labeled peptides (K_d
10
11 (Proxyl/TOAC³⁴⁸-Gt α (340-350)) = 65 μ M).
12
13
14
15
16
17
18

19 References.

- 20
- 21 1. Hubbell, W. L., Gross, A., Langen, R., and Lietzow, M. A. (1998) Recent advances in
22 site-directed spin labeling of proteins, *Curr Opin Struct Biol* 8, 649-656.
- 23 2. Hubbell, W. L., Cafiso, D. S., and Altenbach, C. (2000) Identifying conformational
24 changes with site-directed spin labeling, *Nat Struct Biol* 7, 735-739.
- 25 3. Columbus, L., and Hubbell, W. L. (2002) A new spin on protein dynamics, *Trends*
26 *Biochem Sci* 27, 288-295.
- 27 4. Rabenstein, M. D., and Shin, Y. K. (1995) Determination of the distance between two
28 spin labels attached to a macromolecule, *Proc Natl Acad Sci U S A* 92, 8239-8243.
- 29 5. Altenbach, C., Oh, K. J., Trabanino, R. J., Hideg, K., and Hubbell, W. L. (2001)
30 Estimation of inter-residue distances in spin labeled proteins at physiological
31 temperatures: experimental strategies and practical limitations, *Biochemistry* 40, 15471-
32 15482.
- 33 6. Jeschke, G. (2002) Distance measurements in the nanometer range by pulse EPR,
34 *Chemphyschem* 3, 927-932.
- 35 7. Pannier, M., Veit, S., Godt, A., Jeschke, G., and Spiess, H. W. (2000) Dead-time free
36 measurement of dipole-dipole interactions between electron spins, *J Magn Reson* 142,
37 331-340.
- 38 8. Langen, R., Oh, K. J., Cascio, D., and Hubbell, W. L. (2000) Crystal structures of spin
39 labeled T4 lysozyme mutants: implications for the interpretation of EPR spectra in terms
40 of structure, *Biochemistry* 39, 8396-8405.
- 41 9. Fleissner, M. R., Cascio, D., and Hubbell, W. L. (2009) Structural origin of weakly
42 ordered nitroxide motion in spin-labeled proteins, *Protein Sci* 18, 893-908.
- 43 10. Guo, Z., Cascio, D., Hideg, K., and Hubbell, W. L. (2008) Structural determinants of
44 nitroxide motion in spin-labeled proteins: solvent-exposed sites in helix B of T4
45 lysozyme, *Protein Sci* 17, 228-239.
- 46 11. Guo, Z., Cascio, D., Hideg, K., Kalai, T., and Hubbell, W. L. (2007) Structural
47 determinants of nitroxide motion in spin-labeled proteins: tertiary contact and solvent-
48 inaccessible sites in helix G of T4 lysozyme, *Protein Sci* 16, 1069-1086.
- 49 12. McHaourab, H. S., Lietzow, M. A., Hideg, K., and Hubbell, W. L. (1996) Motion of
50 spin-labeled side chains in T4 lysozyme. Correlation with protein structure and dynamics,
51 *Biochemistry* 35, 7692-7704.
52
53
54
55
56
57
58
59
60

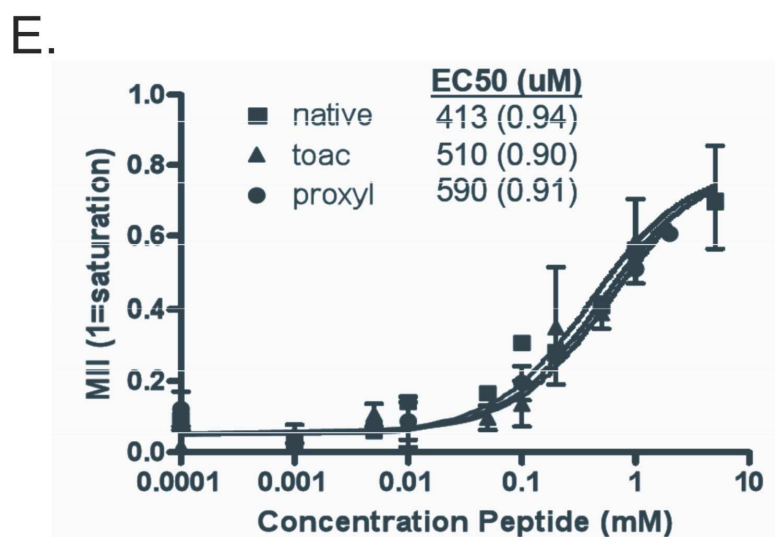
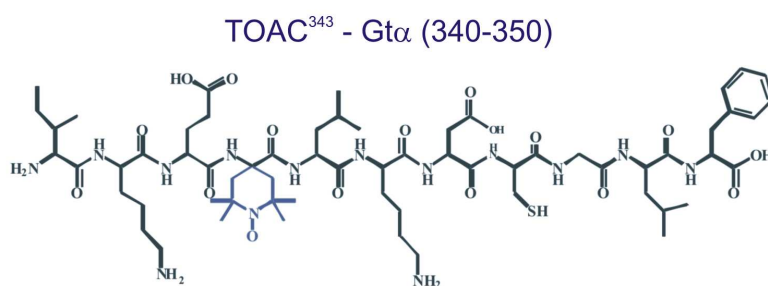
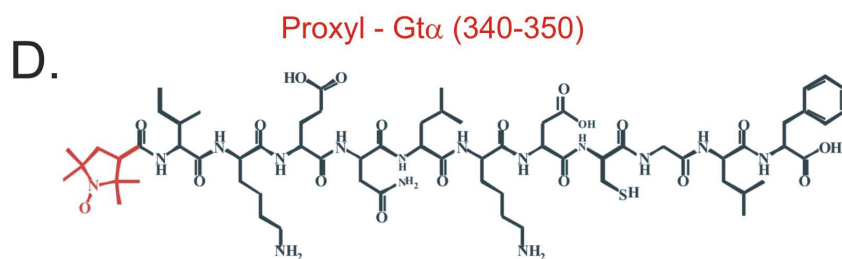
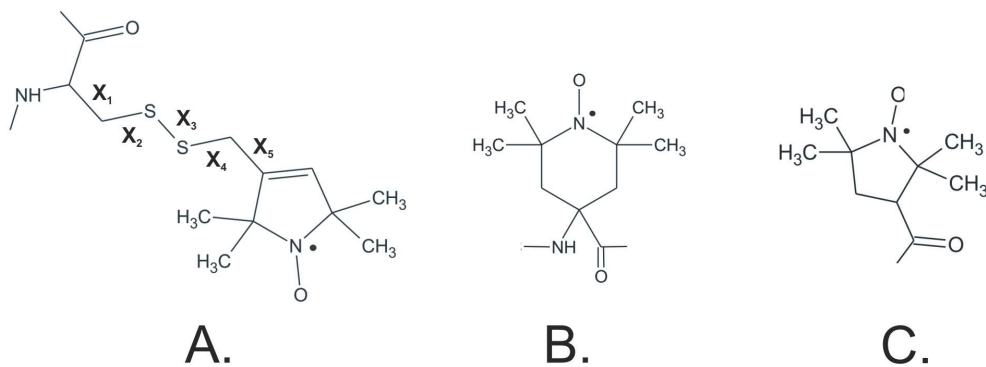
- 1
 - 2
 - 3
 - 4
 - 5
 - 6
 - 7
 - 8
 - 9
 - 10
 - 11
 - 12
 - 13
 - 14
 - 15
 - 16
 - 17
 - 18
 - 19
 - 20
 - 21
 - 22
 - 23
 - 24
 - 25
 - 26
 - 27
 - 28
 - 29
 - 30
 - 31
 - 32
 - 33
 - 34
 - 35
 - 36
 - 37
 - 38
 - 39
 - 40
 - 41
 - 42
 - 43
 - 44
 - 45
 - 46
 - 47
 - 48
 - 49
 - 50
 - 51
 - 52
 - 53
 - 54
 - 55
 - 56
 - 57
 - 58
 - 59
 - 60
13. Lietzow, M. A., and Hubbell, W. L. (2004) Motion of spin label side chains in cellular retinol-binding protein: correlation with structure and nearest-neighbor interactions in an antiparallel beta-sheet, *Biochemistry* *43*, 3137-3151.
14. Columbus, L., Kalai, T., Jeko, J., Hideg, K., and Hubbell, W. L. (2001) Molecular motion of spin labeled side chains in alpha-helices: analysis by variation of side chain structure, *Biochemistry* *40*, 3828-3846.
15. Steinhoff, H.J., Mollaaghabaga, R., Altenbach, C., Hideg, K., Krebs, M., Khorana, H.G., and Hubbell, W.L. (1994) Time-resolved detection of structural changes during the photocycle of spin-labeled bacteriorhodopsin, *Science* *266*, 105-107.
16. Knierim, B., Hofmann K.P., Ernst, O.P., and Hubbell, W.L. (2007) Sequence of late molecular events in the activation of rhodopsin, *Proc Natl Acad Sci* *104*, 20290-20295.
17. Hubbell, W.L., Altenbach, C., Hubbell, C.M., and Khorana, H.G. (2003) Rhodopsin structure, dynamics, and activation: a perspective from crystallography, site-directed spin labeling, sulfhydryl reactivity, and disulfide cross-linking, *Adv Protein Chem* *63*, 243-290.
18. Altenbach, C., Kusnetzow, A. K., Ernst, O. P., Hofmann, K. P., and Hubbell, W. L. (2008) High-resolution distance mapping in rhodopsin reveals the pattern of helix movement due to activation, *Proc Natl Acad Sci U S A* *105*, 7439-7444.
19. Oldham, W.M., Van Eps, N., Preininger, A.M., Hubbell, W.L., and Hamm, H.E. (2007) Mapping allosteric connections from the receptor to the nucleotide binding pocket of heterotrimeric G proteins, *Proc Natl Acad Sci* *104*, 7927-7932.
20. Van Eps, N., Oldham, W.M., Hamm, H.E., and Hubbell, W.L. (2006) Structural and dynamical changes in an alpha-subunit of a heterotrimeric G protein along the activation pathway, *Proc Natl Acad Sci* *103*, 16194-16199.
21. Oldham, W.M., Van Eps, N., Preininger, A.M., Hubbell, W.L., and Hamm, H.E. (2006) Mechanism of the receptor-catalyzed activation of heterotrimeric G proteins, *Nat Struct Mol Biol* *13*, 772-777.
22. Preininger, A.M., Van Eps, N., Yu, N.J., Medkova, M., Hubbell, W.L., and Hamm, H.E. (2003) The myristoylated amino terminus of Galpha(i)(1) plays a critical role in the structure and function of Galpha(i)(1) subunits in solution, *Biochemistry* *42*, 7931-7941.
23. Medkova, M., Preininger, A.M., Yu, N.J., Hubbell, W.L., and Hamm, H.E. (2002) Conformational changes in the amino-terminal helix of the G protein alpha(i1) following dissociation from Gbetagamma subunit and activation, *Biochemistry* *41*, 9962-9972.
24. Hurth, K. M., Nilges, M. J., Carlson, K. E., Tamrazi, A., Belford, R. L., and Katzenellenbogen, J. A. (2004) Ligand-induced changes in estrogen receptor conformation as measured by site-directed spin labeling, *Biochemistry* *43*, 1891-1907.
25. Rassat, A., and Rey, P. (1967) Nitroxides. XXIII. Preparation d'aminoacides radicalaires et de leurs sels complexes, *Bull Soc Chim Fra*, 815.
26. Marsh, D. (2006) Orientation of TOAC amino-acid spin labels in alpha-helices and beta-strands, *J Magn Reson* *180*, 305-310.
27. Crisma, M., Deschamps, J.R., George, C., Flippen-Anderson, J.L., Kaptein, B., Broxterman, Q.B., Moretto, A., Oancea, S., Jost, M., Formaggio, F., and Toniolo, C. (2005) A topographically and conformationally constrained, spin-labeled, alpha-amino acid: crystallographic characterization in peptides, *J Pept Res* *65*, 564-579.

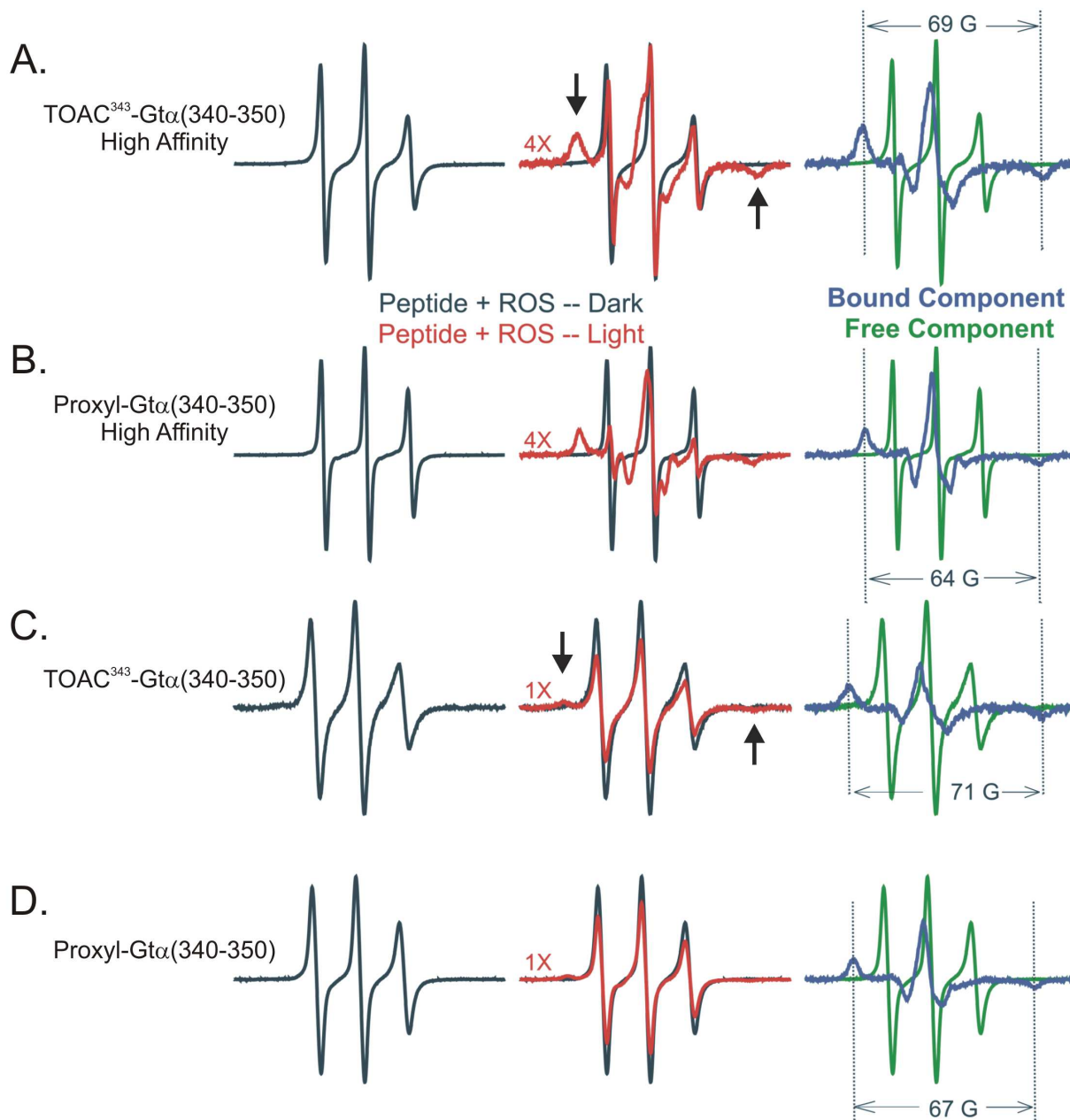
- 1
 - 2
 - 3
 - 4
 - 5
 - 6
 - 7
 - 8
 - 9
 - 10
 - 11
 - 12
 - 13
 - 14
 - 15
 - 16
 - 17
 - 18
 - 19
 - 20
 - 21
 - 22
 - 23
 - 24
 - 25
 - 26
 - 27
 - 28
 - 29
 - 30
 - 31
 - 32
 - 33
 - 34
 - 35
 - 36
 - 37
 - 38
 - 39
 - 40
 - 41
 - 42
 - 43
 - 44
 - 45
 - 46
 - 47
 - 48
 - 49
 - 50
 - 51
 - 52
 - 53
 - 54
 - 55
 - 56
 - 57
 - 58
 - 59
 - 60
28. Schiemann, O., Cekan, P., Margraf, D., Prisner, T. F., and Sigurdsson, S. T. (2009) Relative orientation of rigid nitroxides by PELDOR: beyond distance measurements in nucleic acids, *Angew Chem Int Ed Engl* 48, 3292-3295.
29. Barbosa, S. R., Cilli, E. M., Lamy-Freund, M. T., Castrucci, A. M., and Nakaie, C. R. (1999) First synthesis of a fully active spin-labeled peptide hormone, *FEBS Lett* 446, 45-48.
30. Vesterman, B., Sekacis, I., Betins, J., Podins, L., and Nikiforovich, G. V. (1985) Equilibrium of conformers in solution: spin-labelled angiotensin, *FEBS Lett* 192, 128-130.
31. Nakaie, C. R., Silva, E. G., Cilli, E. M., Marchetto, R., Schreier, S., Paiva, T. B., and Paiva, A. C. (2002) Synthesis and pharmacological properties of TOAC-labeled angiotensin and bradykinin analogs, *Peptides* 23, 65-70.
32. Bettio, A., Gutewort, V., Poppl, A., Dinger, M. C., Zschornig, O., Klaus, A., Toniolo, C., and Beck-Sickinger, A. G. (2002) Electron paramagnetic resonance backbone dynamics studies on spin-labelled neuropeptide Y analogues, *J Pept Sci* 8, 671-682.
33. Smythe, M. L., Nakaie, C. R., and Marshall, G. R. (1995) α -Helical versus 3_{10} -Helical Conformation of Alanine-Based Peptides in Aqueous Solution: An Electron Spin Resonance Investigation, *J Am Chem Soc* 117, 10555-10562.
34. Hanson, P., Martinez, G., Millhauser, G., Formaggio, F., Crisma, M., Toniolo, C., and Vita, C. (1996) *J Am Chem Soc* 118, 271-272.
35. Emeis, D. Kuhn, H., Reichert, J., and Hofmann, K.P. (1982) Complex formation between metarhodopsin II and GTP-binding protein in bovine photoreceptor membranes leads to a shift of the photoproduct equilibrium, *FEBS Letters* 143, 29-34.
36. Sakmar, T. P. (1998) Rhodopsin: a prototypical G protein-coupled receptor, *Prog Nucleic Acid Res Mol Biol* 59, 1-34.
37. Hamm, H. E., Deretic, D., Arendt, A., Hargrave, P. A., Koenig, B., and Hofmann, K. P. (1988) Site of G protein binding to rhodopsin mapped with synthetic peptides from the alpha subunit, *Science* 241, 832-835.
38. Dratz, E. A., Furstenu, J. E., Lambert, C. G., Thireault, D. L., Rarick, H., Schepers, T., Pakhlevanians, S., and Hamm, H. E. (1993) NMR structure of a receptor-bound G-protein peptide, *Nature* 363, 276-281.
39. Kisselev, O. G., Kao, J., Ponder, J. W., Fann, Y. C., Gautam, N., and Marshall, G. R. (1998) Light-activated rhodopsin induces structural binding motif in G protein alpha subunit, *Proc Natl Acad Sci U S A* 95, 4270-4275.
40. Koenig, B. W., Kontaxis, G., Mitchell, D. C., Louis, J. M., Litman, B. J., and Bax, A. (2002) Structure and orientation of a G protein fragment in the receptor bound state from residual dipolar couplings, *J Mol Biol* 322, 441-461.
41. Scheerer, P., Park, J. H., Hildebrand, P. W., Kim, Y. J., Krauss, N., Choe, H. W., Hofmann, K. P., and Ernst, O. P. (2008) Crystal structure of opsin in its G-protein-interacting conformation, *Nature* 455, 497-502.
42. Yang, C. S., Skiba, N. P., Mazzoni, M. R., and Hamm, H. E. (1999) Conformational changes at the carboxyl terminus of Galpha occur during G protein activation, *J Biol Chem* 274, 2379-2385.
43. Oldham, W. M., Van Eps, N., Preininger, A. M., Hubbell, W. L., and Hamm, H. E. (2006) Mechanism of the receptor-catalyzed activation of heterotrimeric G proteins, *Nat Struct Mol Biol* 13, 772-777.

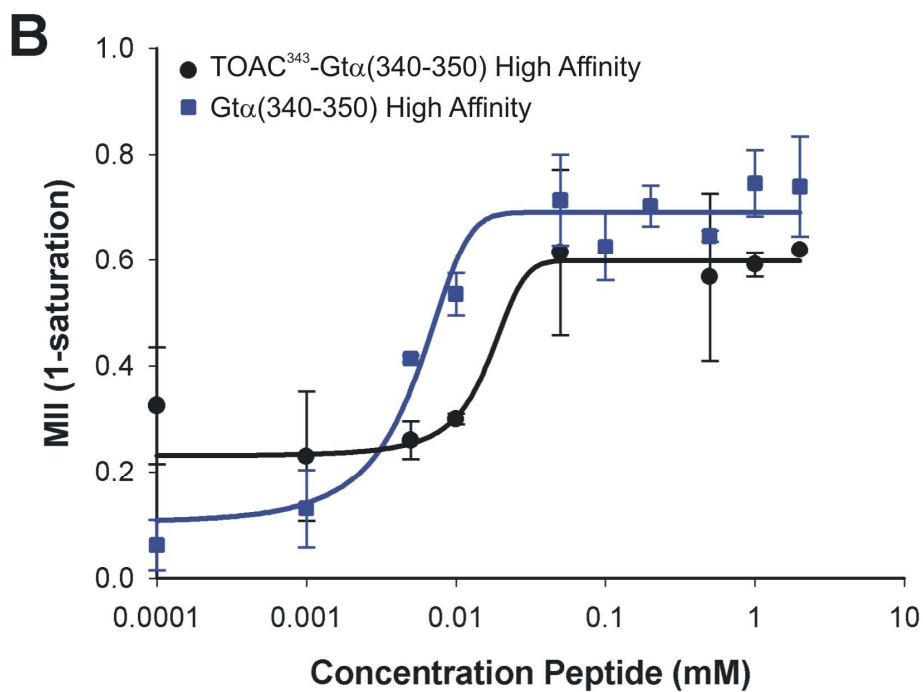
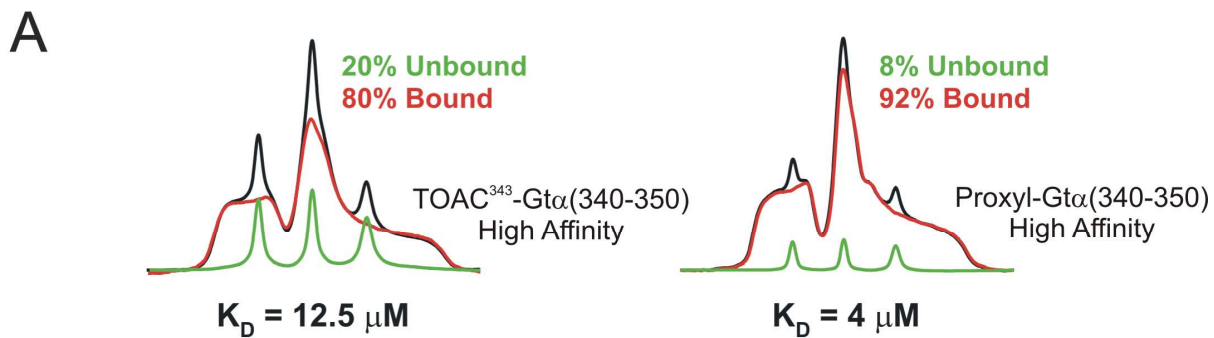
- 1
2
3
4
5
6
7
8
9
10
11
12
13
14
15
16
17
18
19
20
21
22
23
24
25
26
27
28
29
30
31
32
33
34
35
36
37
38
39
40
41
42
43
44
45
46
47
48
49
50
51
52
53
54
55
56
57
58
59
60
44. Martin, E. L., Rens-Domiano, S., Schatz, P. J., and Hamm, H. E. (1996) Potent peptide analogues of a G protein receptor-binding region obtained with a combinatorial library, *J Biol Chem* 271, 361-366.
 45. Smythe, M. L., Nakaie, C. R., and Marshall, G. R. (1995) α -Helical versus 3_{10} -Helical Conformation of Alanine-Based Peptides in Aqueous Solution: An Electron Spin Resonance Investigation, *J. Am. Chem. Soc.* 117, 10555-10562.
 46. Mazzoni, M.R., Malinski, J.A., and Hamm, H.E. (1991) Structural analysis of rod GTP-binding protein, Gt. Limited proteolytic digestion pattern of Gt with four proteases defines monoclonal antibody epitope, *J Biol Chem* 266, 14072-14081.
 47. Kisselev, O., Ermolaeva, M., and Gautam, N. (1995) Efficient interaction with a receptor requires a specific type of prenyl group on the G protein gamma subunit, *J Biol Chem* 270, 25356-25358.
 48. Papermaster, D. S., and Dreyer, W. J. (1974) Rhodopsin content in the outer segment membranes of bovine and frog retinal rods, *Biochemistry* 13, 2438-2444.
 49. Hanson, S. M., Van Eps, N., Francis, D. J., Altenbach, C., Vishnivetskiy, S. A., Arshavsky, V. Y., Klug, C. S., Hubbell, W. L., and Gurevich, V. V. (2007) Structure and function of the visual arrestin oligomer, *EMBO J* 26, 1726-1736.
 50. Arimoto, R., Kisselev, O. G., Makara, G. M., and Marshall, G. R. (2001) Rhodopsin-transducin interface: studies with conformationally constrained peptides, *Biophys J* 81, 3285-3293.
 51. Monaco, V., Formaggio, F., Crisma, M., Toniolo, C., Hanson, P., Millhauser, G., George, C., Deschamps, J. R., and Flippen-Anderson, J. L. (1999) Determining the occurrence of a $3(10)$ -helix and an alpha-helix in two different segments of a lipopeptaibol antibiotic using TOAC, a nitroxide spin-labeled C(alpha)-tetrasubstituted alpha-aminoacid, *Bioorg Med Chem* 7, 119-131.
 52. Toniolo, C., Valente, E., Formaggio, F., Crisma, M., Pilloni, G., Corvaja, C., Toffoletti, A., Martinez, G. V., Hanson, M. P., Millhauser, G. L., and et al. (1995) Synthesis and conformational studies of peptides containing TOAC, a spin-labelled C alpha, alpha-disubstituted glycine, *J Pept Sci* 1, 45-57.
 53. Monaco, V., Formaggio, F., Crisma, M., Toniolo, C., Hanson, P., and Millhauser, G. L. (1999) Orientation and immersion depth of a helical lipopeptaibol in membranes using TOAC as an ESR probe, *Biopolymers* 50, 239-253.
 54. McNulty, J. C., Silapie, J. L., Carnevali, M., Farrar, C. T., Griffin, R. G., Formaggio, F., Crisma, M., Toniolo, C., and Millhauser, G. L. (2000) Electron spin resonance of TOAC labeled peptides: folding transitions and high frequency spectroscopy, *Biopolymers* 55, 479-485.
 55. Freed, J. H. (1976) in *Spin Labeling: Theory and Application* (Berliner, L. J., Ed.), pp 53-132, Academic Press, New York.
 56. Cone, R. A. (1972) Rotational diffusion of rhodopsin in the visual receptor membrane, *Nat New Biol* 236, 39-43.
 57. Heck, M., Schadel, S. A., Maretzki, D., Bartl, F. J., Ritter, E., Palczewski, K., and Hofmann, K. P. (2003) Signaling states of rhodopsin. Formation of the storage form, metarhodopsin III, from active metarhodopsin II, *J Biol Chem* 278, 3162-3169.
 58. Johnston, C. A., and Siderovski, D. P. (2007) Structural basis for nucleotide exchange on G alpha i subunits and receptor coupling specificity, *Proc Natl Acad Sci U S A* 104, 2001-2006.

- 1
2
3
4
5
6
7
8
9
10
11
12
13
14
15
16
17
18
19
20
21
22
23
24
25
26
27
28
29
30
31
32
33
34
35
36
37
38
39
40
41
42
43
44
45
46
59. Kusumi, A., and Hyde, J. S. (1982) Spin-label saturation-transfer electron spin resonance detection of transient association of rhodopsin in reconstituted membranes, *Biochemistry* *21*, 5978-5983.
 60. Downer, N. W., and Cone, R. A. (1985) Transient dichroism in photoreceptor membranes indicates that stable oligomers of rhodopsin do not form during excitation, *Biophysical Journal* *47*, 277-284.
 61. Kisselev, O. G., Meyer, C. K., Heck, M., Ernst, O. P., and Hofmann, K. P. (1999) Signal transfer from rhodopsin to the G-protein: evidence for a two-site sequential fit mechanism, *Proc. Natl. Acad. Sci. U.S.A.* *96*, 4898-4903.
 62. Herrmann, R., Heck, M., Henklein, P., Kleuss, C., Hofmann, K. P., and Ernst, O. P. (2004) Sequence of interactions in receptor-G protein coupling, *J Biol Chem* *279*, 24283-24290.
 63. Arnis, S., and Hofmann, K. P. (1993) Two different forms of metarhodopsin II: Schiff base deprotonation precedes proton uptake and signaling state, *Proc Natl Acad Sci U S A* *90*, 7849-7853.
 64. Mah, T. L., Szundi, I., Lewis, J. W., Jager, S., and Kliger, D. S. (1998) The effects of octanol on the late photointermediates of rhodopsin, *Photochem Photobiol* *68*, 762-770.
 65. Lewis, J. W., Szundi, I., Kazmi, M. A., Sakmar, T. P., and Kliger, D. S. (2006) Proton movement and photointermediate kinetics in rhodopsin mutants, *Biochemistry* *45*, 5430-5439.
 66. Altenbach, C., Yang, K., Farrens, D.L., Farahbakhsh, Z.T., Khorana, H.G., and Hubbell, W.L. (1996) Structural Features and Light-Dependent Changes in the Cytoplasmic Interhelical E-F Loop Region of Rhodopsin: A Site-Directed Spin-Labeling Study, *Biochemistry* *35*, 12470-12478.
 67. Anderson, L. L., Marshall, G. R., and Baranski, T. J. (2005) Expressed protein ligation to study protein interactions: semi-synthesis of the G-protein alpha subunit, *Protein Pept Lett* *12*, 783-787.
 68. Anderson, L. L., Marshall, G. R., Crocker, E., Smith, S. O., and Baranski, T. J. (2005) Motion of carboxyl terminus of Galpha is restricted upon G protein activation. A solution NMR study using semisynthetic Galpha subunits, *J Biol Chem* *280*, 31019-31026.
- 47
48
49
50
51
52
53
54
55
56
57
58
59
60

FIGURES







1
2
3
4
5
6
7
8
9
10
11
12
13
14
15
16
17
18
19
20
21
22
23
24
25
26
27
28
29
30
31
32
33
34
35
36
37
38
39
40
41
42
43
44
45
46
47
48
49
50
51
52
53
54
55
56
57
58
59
60

